Frequency Selective Bolometers - Progress and Projections

G.W. Wilson[a], T.C. Chen[b], E.S. Cheng[c], D.A. Cottingham[b], T.M. Crawford[e],
T. Downes[e], F.M. Finkbeiner[f], D.J. Fixsen[f], D.W. Logan[a],
S. Meyer[e], T. Perera[e], E.H. Sharp[b], and R.F. Silverberg[d]

[a]University of Massachusetts, Dept. of Astronomy, Amherst, MA, 01003, U.S.A.
[b]Global Science and Technology, NASA/GSFC, LASP, Greenbelt, MD, U.S.A.
[c]Conceptual Analytics, Glenn Dale, MD, U.S.A. [d]NASA/GSFC, Greenbelt, MD, U.S.A.
[e]Univ. of Chicago, Chicago, IL, U.S.A.
[f]SSAI, Greenbelt, MD, U.S.A.

ABSTRACT

We describe recent progress in the modeling and production of Frequency Selective Bolometers operating in the frequency range of 150-1500 GHz. The Frequency Selective Bolometer (FSB) functions by incorporating a bolometer element into a resonant structure to control the range of frequencies over which it absorbs. Both the bolometer absorber and the backshort are planar metal layers with periodic patterns that resonate at the desired frequency. The bolometer layer is resistive and absorbs the incident radiation at the desired frequency while the backshort is a low resistivity resonant pattern. The transmission, reflection, and absorption spectra of this two-layer structure are predicted with a numerical model and controlled by the design of the characteristics of the patterns. The key advantage to the FSB bolometer lies in the fact that the radiation not absorbed on the bolometer is transmitted through the device and passed on to subsequent FSB elements that are tuned to other frequencies. Thus a stack of FSB elements enables a multi-spectral single pixel with a geometry that can be close packed into an array of pixels.

We describe the electromagnetic modeling and measurements of FSBs spanning 150 to 1500 GHz. The discussion is focused on two issues: prediction and control of the FSB passband and the projected high frequency limit of FSBs currently being produced. Results from FSBs produced for the SPEctral Energy Distribution (SPEED) receiver (150-350 GHz) are shown along with corresponding results from prototype FSBs for the Explorer of Diffuse high-z Galactic Emission (EDGE) telescope (300-1500 GHz).

Keywords: Bolometer Camera, FIR Detectors, Cosmology, LMT

1. INTRODUCTION

The past five years has witnessed a growing effort by both ground and space-based millimeter and sub-millimeter wave observatories to build large-format bolometer arrays. Pioneering work by the SCUBA team in constructing a 128 element bolometer camera for the JCMT[1] has been followed by the 37 detector MAMBO instrument for the IRAM 30 m telescope, the 144 element BOLOCAM[2] and 384 element SHARC II[3] instruments on the CSO as well as the sub-orbital BLAST arrays (280 elements) and the 270 element SPIRE arrays on the Herschel satellite.[4] With the advent of multiplexed transition-edge superconducting (TES) detectors, this trend of larger detector arrays is expected to continue with several TES arrays currently in the construction phase including the approximately 10,000 element SCUBA II array for the JCMT.[5]

In contrast to these dramatic advances in array size, technologies that efficiently increase the spectral range of bolometer cameras have received relatively little attention. In fact, the cameras above which observe simultaneously in more than one band do so at great expense in complexity, mass, and detector efficiency by combining

---

the beams of multiple monochromatic detector arrays using complex schemes of dichroic filters and re-imaging optics or by sharing the focal plane between detectors illuminated by different feed horns. Instruments limited to one pass band at a time change frequencies either by replacing the upstream filters and array backshort (BOLOCAM) or by utilizing a filter wheel (SHARC II).

Herein we describe our progress in developing the Frequency Selective Bolometer (FSB) technology which addresses the desire for array receivers to spectrally multiplex the large bandwidth available at a telescope focal plane in a compact and efficient manner. This technology is planned to be demonstrated in two future instruments: the SPEctral Energy Distribution (SPEED) camera[6, 7] and the Explorer of high-z Diffuse Galactic Emission (EDGE) experiment.[8] SPEED observes in four bands, between 2.1mm and 0.85mm, simultaneously in four pixels from a ground-based telescope. EDGE is a balloon-borne experiment which will observe in eight bands, from 300 GHz to 1.5 THz, simultaneously in seven pixels.

This paper is organized as follows. In Section 2 we describe the FSB concept and its implementation. In Section 3 we briefly outline the optical modeling of FSBs and show model/measurement comparisons. In Section 4 we describe the fabrication of the detectors with emphasis on the transition-edge superconducting sensors and on the limitations of the current processing for pushing FSBs to high frequencies.

2. FREQUENCY SELECTIVE BOLOMETERS

Traditionally, bolometric continuum detectors have used broad bandwidth absorbers (usually thin sheets of Au or Bi) and have left the definition of the system passband to upstream optics. While this approach results in detectors which can be used to observe different spectral passbands (BOLOCAM and SHARK II), in practice one finds that the optimal detector parameters for a particular passband are a strong function of the total power loading on the detector. Thus, ultra-broad bandwidth detectors only achieve their maximum sensitivity over a much smaller bandwidth of operation.

Frequency selective bolometers utilize a frequency selective surface to define the passband at the detector. Incorporating a pair of resonant arrays of dipole antennas as shown in the inset of Figure 1, the frequency selective bolometer absorbs only over a well defined passband while allowing radiation outside of that band to pass (see Figure 1). The bolometer is backed by a similarly resonant frequency selective backshort, spaced at $\lambda/4$ behind the absorber. The backshort functions to steepen the cutoff of the passband and to increase the coupling efficiency of the bolometer. By cascading a series of FSBs with successively lower passband frequencies, a multi-spectral pixel is created. There are several significant advantages to this design over the broad bandwidth absorber approach:

- The detector array geometry can be compact and light-weight.

- The lack of dichroic and bandpass filters results in a more efficient optical path with fewer elements contributing to scattering.

- Several passbands may be stacked at high efficiency in a single array.

- The system passbands are defined at the detector level, minimizing the complexity of optical alignments and cooling of external filters.

- The detectors are optimized for the passband they are designed to accept.

Over the past two years we have realized a series of prototype frequency selective surfaces and frequency selective bolometers ranging in frequency from 150 GHz to 1.5 THz. Both absorptive (bolometers) and reflective (backshorts) surfaces have been studied in transmission using Fourier Transform Spectrometers (FTS) at the University of Chicago and the University of Massachusetts. All prototype devices were fabricated using the Detector Development Laboratory at the Goddard Space Flight Center. The prototype optical devices were generated in order to test and calibrate our numerical model of frequency selective surfaces (see Section 3). The prototype bolometers were fabricated to explore the thermal properties of large detectors (see Section 4).
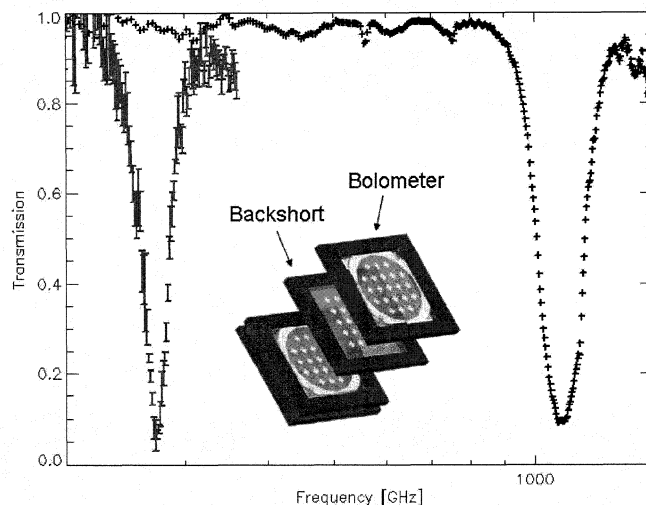
Figure 1. Plot: Transmission of a pair of FSBs. Note that these devices were measured individually, not in a stack configuration. The high low-frequency transmission of the 1150 GHz device (black data points) allows lower frequency FSBs to be placed directly behind yet still achieve high coupling efficiency. Note also that the high frequency FSB will act as a band-stop filter for subsequent lower frequency devices. Inset: A cartoon of an exploded pair of FSBs.

3. MODELING OF FREQUENCY SELECTIVE SURFACES

Significant analytical modeling of frequency selective surfaces dates back to studies of tuned surfaces utilized to diminish the bandwidth of reflectivity of military radar antennas in the 1950s.[9] In the case of this research, optical performance of FSBs is predicted and optimized using Ansoft's High Frequency Simulation Software (HFSS) v.8.5 on a 4 Xeon 1.5 GHz processor computer. HFSS is a finite element solver that calculates Maxwell's equations at all points on a generated mesh.

FSBs are optically large devices and even a simple model of the electric field around a single cross requires a large dynamic range in the solver. To numerically solve the case of an incident plane wave on an FSB, one must mesh the geometry finely enough to accurately represent the fields while not exceeding the memory and processing limits of the computing platform. This places a constraint on the overall range of scales in a given geometry. For our prototype FSBs, the ratio of largest to smallest feature is 2×10^4. To make the problem of modeling an array of crosses tractable, we model a single pair of crosses (an absorbing and a reflecting cross) with periodic boundary conditions that mimic an *infinite* array of cross pairs.* To further simplify the geometry, each cross is modeled as a 2-dimensional structure since the typical thickness of the crosses (0.2μm) is one part in 1000 of the shortest wavelength simulated.

The left side of Fig. 2 shows an exploded cartoon view of a model unit cell. The model consists of each cross located on a surface of 0.5 μm thick silicon nitride and separated by a distance of $\lambda/4$. The ends of the model are capped with a Perfectly Matched Layer (PML) that, by construction, absorbs all the incident radiation and terminates the cavity. The crosses are excited by a plane wave traveling along the z-axis and the transmission and reflection of the cross pair are calculated at the planes labeled "In" and "Out" by integrating the Poynting vector of the scattered fields at these planes. The backshort cross is modeled as a perfect conductor and the absorbing cross is modeled with a sheet resistance of 1.6 Ω/square. The 0.5 μm silicon nitride sheet on which the crosses are laid down is modeled as a finite thickness sheet with a relative permittivity of 7.5.

---

*Modeling a unit cell with periodic boundary conditions restricts the model to the wavelength range $2g \leq \lambda \leq g/2$ where g is the periodicity of the array. For this reason we are only able to model FSBs near their resonance.
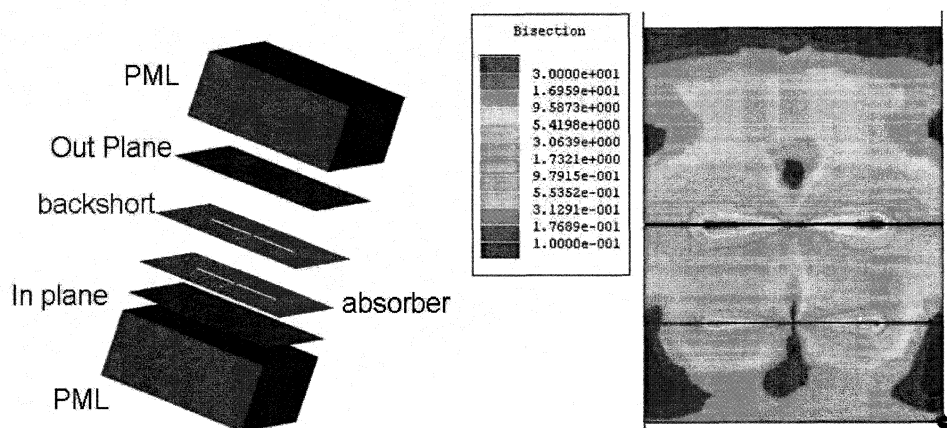
Figure 2. Left: An exploded cartoon view of an FSB unit cell as modeled in Ansoft's HFSS v8.5. Right: Sectional view of the scattered electric field amplitude. The units of the key are V/m.

The right side of Figure 2 shows the scattered electric field distribution for a model at frequencies near the resonance. The coupling of evanescent fields between the bolometer and backshort is clearly visible in the figure. Note that this behavior is not modeled in transmission-line calculations of layered frequency selective surfaces and yet, as shown below, is essential to accurately predicting the spectral response of the surfaces.

3.1. Models and Measurements

We have fabricated a series of FSB prototype devices to test the validity of the HFSS model. Optical models of frequency selective surfaces were produced at the NASA/GSFC Detector Development Laboratory and measured in transmission at the University of Chicago. We designed these devices to have physical properties as similar as possible to those desired for the SPEED and EDGE detectors so that we could both test the GSFC fabrication process and the frequency selective surface modeling.

The optical models were made on 200 μm silicon wafers coated with a 0.5 μm silicon nitride film. In all cases the active surface of the test devices was 1 cm in diameter, circumscribed by a 1.2 cm square (inside dimension) Si frame. The devices are mounted in a 1 cm light pipe which is fed with a pair of back to back Winston cones (4.5 mm^{2}sr or 14 mm^{2}sr) which serve to define the throughput of the incident radiation. The pair of cones was illuminated by a Fourier Transform Spectrometer. A 4K bolometer downstream of the test devices measured the transmitted radiation. Since this setup is inherently uncalibrated, all measurements are the ratio of the transmitted power with and without the test devices in the setup.

Below we describe results of this testing with emphasis on aspects related to the scaling of FSBs to THz frequencies.

Bolometer/Backshort Alignment

We have empirically demonstrated the importance of the modeled evanescent field coupling between the absorber and backshort layers to the passband shape by measuring actual FSBs with the bolometer intentionally misaligned with the backshort. As shown at left in Figure 3, misalignment of the surfaces causes significant deviations in the spectral behavior of the device. This set of empirical tests shows that for narrow transmission profiles the relative cross alignment must be better than $g/4$ where g is the periodicity of the cross array. For an FSB at 1.5 THz, $g/4 \sim 38\mu$m which should be straightforward to achieve under a microscope.

Scaleability of FSBs

To test the frequency range of the FSB production process a series of four prototype devices ranging from 0.2 to 1.1 THz was fabricated and tested in transmission. Model and measurement results are shown for these devices
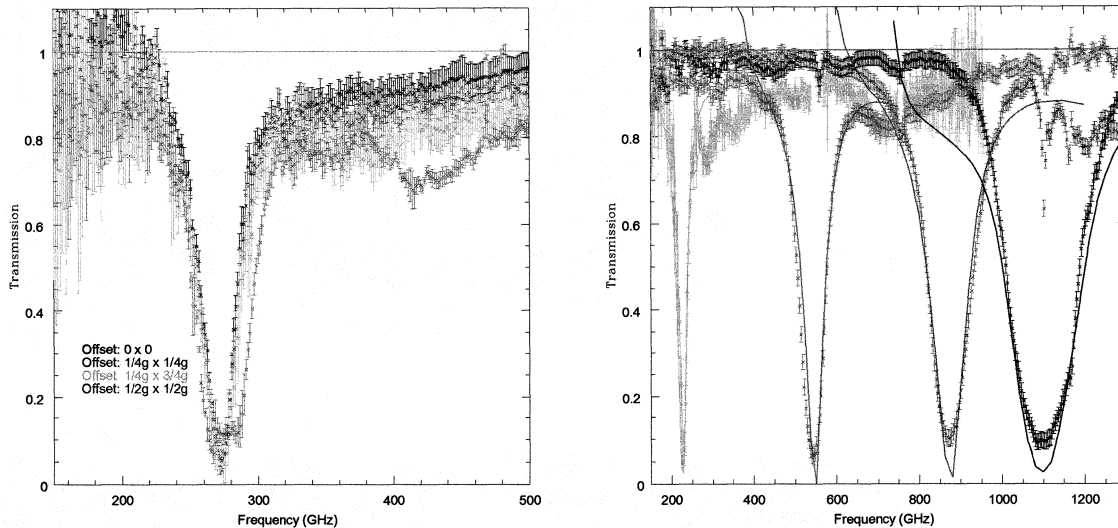
Figure 3. Left: Transmission of a 270 GHz FSB with four alignments of the bolometer and backshort layers. Significant deviation from the aligned case is seen for misalignments greater than $g/4$. Right: Transmission responses of FSBs tuned to different resonant frequencies from 0.2 to 1.1 THz.

in Figure 3. As expected, the transmission of the FSBs far from resonance approaches unity. Unfortunately, we were not aware of the importance of layer alignment at the time of measurement and the relative alignment of layers is nearly random. Thus, the asymmetry in the transmission between the low and high frequency sides of the resonance is likely due to misalignments though we can not yet rule out a contribution from additional mode coupling due to the finite optical opening angle of the lightpipe. Note however that the passband shapes shown in Figure 3 are already suitable for continuum measurements from balloon-borne platforms such as the EDGE experiment.

Qualitatively the predicted transmission of the FSBs matches the measured transmission closely through the resonance. The deviations between the model and the measurements illuminate the shortcomings of the model and the challenges of assembling FSBs at THz frequencies. Although it is possible to tweak individual models to better match the observed spectra, the power of the HFSS model is to predict the bandpass of many such FSBs without fabricating many prototype devices. By creating simulations, we are able to efficiently explore a wide range of parameters and designs for the optical behavior of future FSBs.

4. BOLOMETER DESIGN

In parallel with the optical prototype devices described above we have fabricated complete bolometer elements to test the thermal properties of the FSBs *independently* of their optical properties. This process included the development of a new approach to constructing TES sensors[10, 11] as well as new techniques to fabricate large free-standing membranes of silicon nitride. Figure 4 shows a prototype bolometer. Below we describe these prototype bolometers along with the challenges we are now working to overcome.

The cross arrays for both the bolometers and backshorts are in the same design as for the test pieces referred to in the previous section. The crosses are made of gold on a 0.5 μm silicon nitride substrate. The gold on the backshorts is 200 nm thick, to give high conductivity; on the bolometers it is 20 nm, which tunes it to optimum absorptivity. In both cases the gold is patterned using a lift-off process. This gives much sharper edge definition than a gold-etch process; the edge definition is important because the currents are highest near the edges of the gold and degradation of conductivity there would result in degradation of the passbands.

For the bolometers, the absorbing area must be partially thermally isolated from the frame temperature. This is achieved by a reactive ion etch of the silicon nitride film to cut it away from the frame except for four

narrow legs. In addition, because the thin nitride film tends to curl, additional support legs are formed to maintain an appropriate tension in the film.

The temperature of the absorber is sensed with TES sensors placed outside the optical path. The prototypes have two TES sensors located on opposite edges of the disk. The sensors are formed of Au/Mo. Our current prototypes use the Mo layer as the electrical leads, bolstered with additional sputtered Mo on top. The leads run down the support legs to the frame, where they terminate in bonding pads. The leads are the primary thermal conduction path from the disk to the frame, and are thus the primary contributor to the bolometer G.

Silicon nitride is not a very good thermal conductor, and this has led to some challenges in the prototype bolometers. In the classical model of a bolometer, the absorber disk is perfectly isothermal, and the bolometer can therefore be modeled as a heat capacity C connected to the thermal bath through a conductivity G. If the absorber is not isothermal, two general problems arise. First, if the conductivity across the disk is not much greater than the conductivity down the legs then the temperature signal at the TES is attenuated and the sensitivity is decreased. Second, if the characteristic thermal time constant of the disk is not short compared to the bolometer time constant there is additional thermal noise; in the literature this is often referred to as a "hanging heat capacity." A third problem more specific to our situation is that poor conduction across the disk leads to electrical response of the TES out to high post detection frequencies; if this response continues into the vicinity of $f \approx R/(2\pi L)$, where L is the SQUID inductance and R is the TES resistance, an instability occurs. These problems are exacerbated in our case by the fact that we are designing these bolometer for ground-based telescopes, where the high background environment forces a high G.

All three problems clearly could be resolved by using a different substrate with higher conductivity, such as Si. However, this would give up the advantage of the low optical impact of the various silicon nitride sheets in the optical path. To mitigate the problems described above in our prototypes, we are experimenting with a gold ring that outlines the optically active portion of the bolometer. This ensures that at least the part of the bolometer outside the optical path is isothermal. It of course does nothing about the first problem listed above, but potentially can solve the other two by adding enough heat capacity in contact with the TES to slow the devices down to the point where the "hanging heat capacity" will not contribute noise, and the SQUID instability is not reached. Note that, unlike traditional semiconducting bolometers, these devices are sufficiently fast due to their electrothermal feedback that one can choose to slow the devices by a factor of 10 without impacting operational performance at the telescope.

5. CONCLUSION

We have described recent progress in the modeling and implementation of frequency selective bolometers. The construction and characterization of prototype optical devices and of prototype bolometers has revealed non-
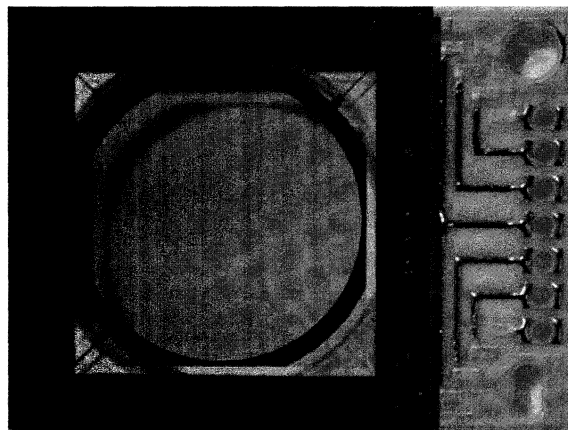

Figure 4. Photograph of an FSB bolometer layer.

intuitive characteristics of the devices which are now accounted for in the optical and thermal models. At present, there appears to be no significant roadblock to the implementation of FSBs at THz frequencies, though at some frequency above 1.5 THz we expect that the limitations in the lift-off process will limit the quality of the device passband.

ACKNOWLEDGMENTS

REFERENCES

1. W. S. Holland, C. R. Cunningham, W. K. Gear, T. Jenness, K. Laidlaw, J. F. Lightfoot, and E. I. Robson, "SCUBA: a submillimeter camera operating on the James Clerk Maxwell Telescope," in *Proc. SPIE Vol. 3357, p. 305-318, Advanced Technology MMW, Radio, and Terahertz Telescopes, Thomas G. Phillips; Ed.*, pp. 305–318, July 1998.
2. J. Glenn, P. A. R. Ade, M. Amarie, J. J. Bock, S. F. Edgington, A. Goldin, S. Golwala, D. Haig, A. E. Lange, G. Laurent, P. D. Mauskopf, M. Yun, and H. Nguyen, "Current status of Bolocam: a large-format millimeter-wave bolometer camera," in *Millimeter and Submillimeter Detectors for Astronomy. Edited by Phillips, Thomas G.; Zmuidzinas, Jonas. Proceedings of the SPIE, Volume 4855, pp. 30-40 (2003).*, pp. 30–40, Feb. 2003.
3. C. D. Dowell, C. A. Allen, R. S. Babu, M. M. Freund, M. Gardner, J. Groseth, M. D. Jhabvala, A. Kovacs, D. C. Lis, S. H. Moseley, T. G. Phillips, R. F. Silverberg, G. M. Voellmer, and H. Yoshida, "SHARC II: a Caltech submillimeter observatory facility camera with 384 pixels," in *Millimeter and Submillimeter Detectors for Astronomy. Edited by Phillips, Thomas G.; Zmuidzinas, Jonas. Proceedings of the SPIE, Volume 4855, pp. 73-87 (2003).*, pp. 73–87, Feb. 2003.
4. M. J. Griffin, B. M. Swinyard, and L. G. Vigroux, "SPIRE - Herschel's Submillimetre Camera and Spectrometer," in *IR Space Telescopes and Instruments. Edited by John C. Mather. Proceedings of the SPIE, Volume 4850, pp. 686-697 (2003).*, pp. 686–697, Mar. 2003.
5. W. S. Holland, W. Duncan, B. D. Kelly, K. D. Irwin, A. J. Walton, P. A. R. Ade, and E. I. Robson, "SCUBA-2: a new generation submillimeter imager for the James Clerk Maxwell Telescope," in *Millimeter and Submillimeter Detectors for Astronomy. Edited by Phillips, Thomas G.; Zmuidzinas, Jonas. Proceedings of the SPIE, Volume 4855, pp. 1-18 (2003).*, pp. 1–18, Feb. 2003.
6. G. Wilson, T. C. Chen, E. S. Cheng, D. A. Cottingham, T. Crawford, D. J. Fixsen, F. M. Finkbeiner, D. W. Logan, S. Meyer, R. F. Silverberg, and P. T. Timbie, "Spectral energy distribution camera for the LMT," in *Millimeter and Submillimeter Detectors for Astronomy. Edited by Phillips, Thomas G.; Zmuidzinas, Jonas. Proceedings of the SPIE, Volume 4855, pp. 583-593 (2003).*, pp. 583–593, Feb. 2003.
7. D. A. Cottingham, A. Bier, B. Campano, T. C. Chen, E. S. Cheng, T. Crawford, F. M. Finkbeiner, D. J. Fixsen, D. W. Logan, S. Meyer, E. Sharp, R. F. Silverberg, and G. Wilson, "Development of frequency selective bolometers for ground-based MM-wave astronomy," in *Millimeter and Submillimeter Detectors for Astronomy. Edited by Phillips, Thomas G.; Zmuidzinas, Jonas. Proceedings of the SPIE, Volume 4855, pp. 192-200 (2003).*, pp. 192–200, Feb. 2003.
8. S. S. Meyer, E. S. Cheng, D. A. Cottingham, D. J. Fixsen, L. Knox, R. F. Silverberg, P. T. Timbie, and G. Wilson, "The EDGE Project," in *Airborne Telescope Systems II. Edited by Ramsey K. Melugin, Hans-Peter Roeser . Proceedings of the SPIE, Volume 4857, pp. 204-216 (2003).*, pp. 204–216, Feb. 2003.
9. B. Munk, *Frequency Selective Surfaces: Theory and Design*, John Wiley & Sons, Inc., 2000.
10. T. C. Chen, A. Bier, B. A. Campano, D. A. Cottingham, F. M. Finkbeiner, C. O'Dell, E. Sharp, R. F. Silverberg, and G. W. Wilson, "Development of molybdenum-gold proximity bilayers as transition edge sensors for the speed camera," in *Nuclear Instruments and Methods in Physics Research Section A: Accelerators, Spectrometers, Detectors and Associated Equipment*, 2003.

11. R. F. Silverberg, S. Ali, A. Bier, B. A. Campano, T. C. Chen, E. S. Cheng, D. A. Cottingham, T. M. Crawford, T. Downes, F. M. Finkbeiner, D. J. Fisxen, D. Logan, S. S. Meyer, C. O'Dell, T. Perera, E. Sharp, P. T. Timbie, and G. W. Wilson, "A bolometer array for the spectral energy distribution (speed) camera," in *Nuclear Instruments and Methods in Physics Research Section A: Accelerators, Spectrometers, Detectors and Associated Equipment*, 2003.